OPTIMIZATION OF THE EXTRACTION AND PREPARATION OF CELLULOSE MICROFIBERS FROM RICE HUSK USING A FULL FACTORIAL EXPERIMENT

DANIEL FERNANDO HINCAPIÉ ROJAS,[*] TAYRON RONNIE ROMERO RODRIGUEZ,[*] DIANA FERNANDA ORTEGA SOLARTE,[*] OSCAR MOSCOSO LONDOÑO,[*] CESAR LEANDRO LONDOÑO CALDERÓN[*] and ASTRID LORENA GIRALDO[**]

[*]*Departamento de Física y Matemáticas, Universidad Autónoma de Manizales, Manizales, Caldas, Colombia*

[**]*Centro de Investigación y de Estudios Avanzados del Instituto Politécnico Nacional Unidad Querétaro, Libramiento Norponiente 2000, 76230 Querétaro, México*

✉ *Corresponding author: D. F. Hincapié Rojas, daniel.hincapier@autonoma.edu.co*

Received January 24, 2024

Cellulose is one of the most abundant biopolymers on Earth and is of most significant interest due to its properties and uses. Cellulose can be obtained from agro-industrial residues, such as rice husk, whose cellulose content is approximately 30%. In this study, cellulose microfibers were extracted from rice husks. Fibers were obtained by submitting the biomass to alkali (NaOH) and bleaching treatments. These treatments have already been reported in the literature; however, variables such as the concentration of reagents, the time, and the temperature of the chemical treatment have yet to be optimized. A factorial design of experiments with 3 factors and 2 levels for each factor was proposed to optimize the chemical processes. It was determined through the analysis of variance (ANOVA) that the factors evaluated significantly influenced the elimination of non-cellulosic compounds, and that the chemical treatment was more efficient when the factors took high level values. Ultraviolet-visible spectroscopy (UV-Vis) analysis showed the successful removal of undesired components during the alkaline treatment. The effect of the treatments on the morphology upon removing hemicelluloses, lignin, and inorganic material was evaluated through Scanning Electron Microscopy (SEM). The increase in the thermal stability in the alkali-treated rice husk and in cellulose microfibers, compared to the raw rice husk, was established by thermogravimetric analysis (TGA). X-ray diffraction (XRD) indicated that the treatments increased the percentage of crystallinity.

Keywords: cellulose microfibers, rice husk, alkaline treatment, bleaching process, design of experiments

INTRODUCTION

The population growth implies that more resources must be used to guarantee a decent quality of life. From this, many other problems originate, increasing the exploitation of non-renewable sources, such as oil and water, leading to the deterioration and contamination of terrestrial and aquatic ecosystems.[1-4] One of these problems is associated with the agro-industrial sector because of the predominance of monocultures, and the waste generated by these.[5-6] That is why, many current investigations focus on recovering agricultural residues and turning them into value-added products, taking advantage of benefits such as low cost and accessibility.

Rice is one of the most widely consumed cereals worldwide, it is cultivated in humid areas, and its yield depends on climatic conditions and the technology used.[7-9] According to the Food and Agriculture Organization of the United Nations (FAO), the global rice production in 2022 was estimated to be 525.5 million tons,[10] while the husk, an agro-industrial waste, represents approximately 20% of the total weight of the rice grain. The rice milling industry in Colombia generates a considerable quantity of rice husk (RH) during the paddy milling process from the fields. This residue reached 2 million tons in the second semester of 2022.[11] Agro-industrial residues such as rice husk (RH) are sources of

lignocellulosic biomass, and can be used for the production of fertilizer, animal feed, or the generation of biofuels.[12-13] However, most of this biomass is burnt or thrown into water sources, causing hazards and contamination of water sources and the environment, altering soil conditions or emitting harmful gases.[14] RH is made up of organic and inorganic materials; the main lignocellulosic components being cellulose (36-40%), hemicelluloses (12-19%), and lignin (20%), along with metallic oxides, such as silica, which is responsible for its low biodegradability, which causes it to accumulate in the environment.

In nature, cellulose is linked to hemicelluloses and lignin, and generally provides support and rigidity to cellular structures. This polymer is composed of millions of glucose units arranged linearly and is linked by β-(1,4) glycosidic bonds.[15] Its hydrophilicity and biodegradability are among the main characteristics of this biomaterial.[16] Therefore, cellulose microfibers can be used as an additive to improve the properties of materials with applications in construction, textiles, packaging, pharmaceuticals, and cosmetics, among others. Currently, the synthesis of cellulose from agricultural residues has become a topic of great interest, given the growing interest in the development of environmentally friendly materials by environmentally sustainable processes, in line with the concept of circular economy of "innovation for sustainable growth" in the United Nations Sustainable Development Goals (SDGs).

In the literature, different biomass sources have been investigated for the extraction of cellulose, for example, coconut shell,[17] sugarcane bagasse,[18] cassava bagasse,[19] and oil palm residues,[20] soybean pods,[21] wheat straws, soybean husks,[22] corn cob,[23] and rice hulls.[24] Various methods have been reported in the literature to extract cellulose[25-34] from these residues. According to Johar *et al*.,[25] implementing chemical processes, such as alkaline treatment with 4% sodium hydroxide (NaOH) and bleaching with 1.7% sodium chlorite, removes lignin and hemicelluloses. Rashid *et al*.[28] used 3% NaOH for the same treatment, and Hafid *et al*.[33] used 5% NaOH. Concerning bleaching, Ping Lu *et al*.[34] used 1.4% $NaClO_2$, while Bigliardi *et al*.[30] used 1.7% $NaClO_2$. Moreover, high-intensity ultrasonics, high-pressure homogenization, crippling, micro-fluidization techniques, and steam explosion[35] have been used to isolate cellulose.

As various extraction processes have been reported for obtaining cellulose microfibers from RH, it is essential to determine the optimal conditions for the specific treatments to be employed. This study aims to standardize and optimize the removal of lignin, hemicelluloses, and other components, such as pectin and ash, among others, from the rice husk structure, allowing the defibrillation of the cellulose through chemical treatments, such as alkaline treatment and bleaching. For this selective separation, sodium hydroxide and sodium hypochlorite were mainly used. The reactive concentration was optimized in each treatment, as well as the reaction time and temperature. An analysis of variance (ANOVA) was performed to determine the optimal conditions that maximize the response variable (elimination of non-cellulosic components). In ANOVA, experiments are performed systematically in a series of tests (runs). Its design tests all possible combinations between factors and their variation levels.[36-37] The effect of chemical treatment on the crystallinity, thermal properties, surface morphology, functional groups, lignin content, and physicochemical properties of cellulose was critically discussed through the results obtained from X-ray diffraction (XRD), thermogravimetric analysis (TGA), scanning electron microscopy (SEM), and Fourier Transform Infrared (FTIR) and UV-Vis spectroscopy techniques, respectively. Therefore, a thorough study of this process will provide an in-depth understanding of the effectiveness of the alkaline treatment and bleaching process in extracting cellulose from RH.

EXPERIMENTAL

Materials

Sodium hydroxide (99% purity) was used for alkaline treatment. In addition, sodium hypochlorite (15% w/v pure NaClO) and acetic acid (CH_3COOH 5% w/v purity) were used as bleaching agents. All chemicals were purchased from Amoquimicos Colombia S.A.S. and were used without further purification.

Cellulose extraction from rice husk

Mechanical pretreatment

RH was washed with distilled water to remove dust and any other contaminants. Then, it was dried at 100 °C for 3 h. After that, the RH was milled to reduce the particle size of the sample. Finally, the ground RH was sieved in a mesh sieve No. 10 (ø < 2mm) to obtain a fine powder and standardize the process conditions.

Alkaline treatment

The alkali treatment was performed to purify the cellulose by removing lignin and hemicelluloses from RH fibers, following a modified methodology described elsewhere.[26] Accordingly, 5 g of RH was mixed in the sodium hydroxide solution and transferred into a round bottom flask. The treatment was performed at reflux temperature on a hot plate magnetic stirrer at 100 rpm.

For this process, a 2^3 factorial design of experiments was proposed, keeping a sample-solution ratio of 1:20 constant. The factors and levels of the design of experiments were the following: temperature – 80 °C or 100 °C, time – 90 min or 120 min, and sodium hydroxide concentration – 4 wt% or 8 wt%. The parameters are summarized in Table 1.

Once this process was finished, the material was washed five times with distilled water until a neutral pH was reached; and then it was dried for 24 h at 90 °C.

Bleaching treatment

The bleaching treatment was carried out on the alkali-treated RH obtained in the previous step. In this process, the bonds of the chromophore groups are broken, which are responsible for the yellow color of the cellulose,[26] and the purpose is cellulose defibrillation. A 2^3 factorial design was proposed to perform this process keeping the 1:20 ratio (sample:solution) constant. The factors used in these processes were also reagent concentration, temperature, and reaction time. Throughout the process, a constant agitation was maintained, varying the temperature to 70 °C or 90 °C and reaction time of 30 or 60 min; the concentration of the solution was NaClO at 1.7% v/v or 2.3% v/v and CH_3COOH at 1.5% v/v. The obtained paste was washed six times with distilled water until a neutral pH was reached. Finally, the samples were dried for 24 h at 90 °C. For bleaching, most studies use sodium chlorite as a chemical reagent, which is very expensive and difficult to access. Therefore, it was decided to evaluate the efficiency of sodium hypochlorite in this treatment.[32]

NaClO is a bleaching and oxidizing agent widely used to remove impurities, lignin, and hemicelluloses from cellulose. Combined with CH_3COOH, it can eliminate unwanted compounds from cellulose fibers, while maintaining the solution's pH level between 7 and 8. Adding CH_3COOH also helps protect the structure of cellulose fibers during the extraction process from rice husk.

Characterization of cellulose microfibers

Scanning electron microscopy (SEM)

For the morphology study of RH, alkali-treated RH, and cellulose microfibers, the SEM JEOL JSM 5910 LV equipment was used, with a magnification range from 100X to 600X in a high vacuum environment, with accelerating voltages of 15 kV. Before measurements, a gold layer (20 nm thickness approximately) was deposited by sputtering on samples to make them conductive, finally the powdered samples were mounted on adhesive carbon. The ImageJ® software was used to process the images and build the histograms with data obtained from different micrographs from each sample.

Thermogravimetric analysis (TGA)

The thermal measurements of the samples (RH, alkali-treated RH, and cellulose microfibers) were performed by the thermogravimetric analyzer (Themys ONE) equipment, and the data were analyzed using thermogravimetric analysis (TGA) and derivative thermogravimetric analysis (DTGA). The samples were heated at 10 °C/min under an N_2 atmosphere from room temperature to 700 °C. This analysis was carried out to evaluate the thermal stability of the materials and determine the percentage of mass loss (%) due to decomposition and dehydration.

X-ray diffraction (XRD)

The X-ray diffraction technique was used to identify the phases present in the samples (RH, alkali-treated RH, and cellulose microfibers). The samples were pulverized and sieved to obtain homogeneous powders. The diffraction patterns were obtained using the XRD diffractometer Rigaku DMax 2100, using monochromatic CuKα radiation (λ = 1.5406 Å), operating at 30 kV and 20 mA. XRD patterns were recorded between 4 and 50° on a 2θ scale in steps of 0.02 °/s. The method used to obtain the crystallinity index % of the samples was described previously.[44] Briefly, it consists in measuring the intensities of the crystalline peaks and the amorphous area, and using Equation 1, to calculate the crystallinity index value:

$$crystallinity\ index\ \% = \frac{I_{002} - I_{am}}{I_{002}} * 100\% \quad (1)$$

where I_{002} and I_{am} are the maximum intensities of crystalline and amorphous materials, respectively.[25] The diffraction peak for the (002) plane is located at a diffraction angle around 2θ = 22º, and the intensity scattered by the amorphous part is measured as the lowest intensity at a diffraction angle around 2θ = 18º.

Ultraviolet–visible spectroscopy (UV-VIS)

UV-Vis spectroscopy was used to determine the presence of lignin molecules in the remaining solution obtained after the alkaline treatment. The absorbance level of each sample was correlated with the efficiency of the different experimental processes (Table 2) in removing non-cellulosic material. Two solutions were prepared, the first one is the blank of the solvent, and the other is the supernatant obtained from each one of the alkaline treatments. The solutions were arranged in quartz sample holders and passed to the spectrophotometer (Spectroquant Prove 600 UV/Vis spectrophotometer Merck KGaA) to measure their

absorbance at wavelengths ranging from 190 nm to 500 nm with a step of 1 nm per second.

Fourier Transform Infrared Spectroscopy (FTIR)

Fourier Transform Infrared (FTIR) spectra were collected with the diffuse reflectance technique and attenuated total reflectance in a Perkin-Elmer® Spectrum™ GX brand spectrometer in the range of 400–4000 cm^{-1} with a resolution of 4 cm^{-1} and 24 scans. This method was used to identify the vibrational modes present in RH, alkali-treated RH, and cellulose samples.

Design of experiments

The design of experiments (DOE) allowed the establishment of cause–effect relations for the alkaline treatment and bleaching treatment. Two 2^3-factorial DOE with three factors and two levels in each factor was evaluated. The chemical concentrations, temperature, and reaction times were the factors proposed. The evaluated response variables were the mass losses in all cases. The experiments were done in quadruplicate. Information on the factors and levels proposed in the alkaline treatment and bleaching process is summarized in Table 1.

The linear regression model equation was obtained through statistical analysis; for this, the Minitab® software version 18 was used.[45] In this study, 5% was defined for the significance level; the null hypothesis (H_0) establishes that the factors of the experiment do not have a significant effect on the synthesis of cellulose microfibers, while the alternative hypothesis (H_1) establishes that the factors show statistically significant differences. In addition, the three assumptions of the ANOVA will be analyzed (normality, homoscedasticity, and the independence of the data). Finally, Tables 2 and 3 show the random order of the runs defined for the alkaline treatment and the bleaching process, respectively.

Finally, to calculate the mass losses in each of these runs, an Analytical Balance PCE-ABE220 with a precision of ±0.0001 g, which allowed determining mass loss after the alkali treatment and bleaching processes, was used. For the mass loss percentage (ML) calculation, Equation 2 was applied, where (M_o) is the initial mass and (M_f) is the final mass after the chemical process:

$$ML = \frac{Mo - Mf}{Mo} * 100\% \quad (2)$$

RESULTS AND DISCUSSION

The methodology proposed here removes the hemicelluloses, lignin, and silica from RH in two steps: at first, the lignin, hemicelluloses and silica are removed with an alkaline sodium hydroxide solution, and then the cellulose pulp is bleached by adding sodium hypochlorite and acetic acid to the solution to purify the cellulose microfibers.

Table 1
Specifications of DOE performed for alkali treatment and bleaching, with their factors, levels, response variables (R), and number of replicates

DOE	Type	Factors and levels						Response variable	Replicates
		A		B		C			
Alkaline treatment	2^3 DOE Factorial	NaOH %(w/v)		Temperature (°C)		Time (min)		Mass loss (%)	4
		4	8	80	100	90	120		
Bleaching	2^3 DOE Factorial	NaClO and CH_3COOH % (v/v)		Temperature (°C)		Time (min)		Mass loss (%)	4
		1.7	2.3	70	90	30	60		

Table 2
Random runs of alkaline treatment

Experiment	Number of runs				NaOH (%)	Time (min)	Temperature (°C)
1	4	9	17	23	4	90	100
2	3	7	21	31	4	90	80
3	11	12	19	29	8	90	100
4	5	16	25	32	8	90	80
5	6	8	18	30	4	120	100
6	2	10	14	26	4	120	80
7	13	15	20	22	8	120	80
8	1	24	27	28	8	120	100

Table 3
Random runs of bleaching treatment

Experiment	Number of runs				NaClO (%)	Time (min)	Temperature (°C)
1	13	15	20	28	1.7	60	70
2	1	4	11	5	2.3	60	70
3	6	10	16	27	1.7	60	90
4	2	9	14	22	2.3	60	90
5	8	18	21	23	1.7	30	70
6	3	7	12	31	2.3	30	70
7	19	24	26	32	1.7	30	90
8	17	25	29	30	2.3	30	90

Physical characterization: mass loss percentages

For delignification with NaOH, the treated RH was recovered on the basis of 5.00 g of the initial dry sample. Approximately 2.15–2.72 g of sample was recovered after delignification according to the experimental conditions in Table 1. This corresponds to a mass recovery of 42.8% and 54.3%, respectively. For cellulose purification with NaClO and CH_3COOH, the alkali treated RH was recovered based on 5.00 g of the initial dry sample. Approximately 1.98–2.99 g of samples was recovered after the bleaching process according to the experimental conditions in Table 1. This corresponds to a mass recovery of 39.60% and 59.80%, respectively. In terms of the percentage mass losses of the alkaline treatment and the bleaching process, the experiment that eliminated the largest amount of mass is number 8; where the three factors (concentration, temperature and reaction time) were at the high level. On the other hand, the experiment that has the highest percentage of mass elimination in the bleaching process is number 4, where the three factors are also at the high level. The reproducibility of the experiments is shown by the low deviation of the data for both treatments.

Ultraviolet–visible spectroscopy (UV-Vis)

The alkali treatment has been used to purify cellulose microfibers by dissolving hemicelluloses and lignin compounds. The UV-Vis technique was used to determine the presence of lignin in the solution obtained after alkali process. These results were correlated with the efficiency of the different experimental processes in removing non-cellulosic material. Figure 1a shows the relationship between the percentage of mass loss and the absorbance by UV-Vis for each of the experiments of the alkaline treatment according to the experimental conditions listed in Table 2. In accordance with the distribution of the data, there can be distinguished three groups of relationships.

Group 1 includes experiments 1, 2, 4 and 6, which have the lowest absorption values between 2.26-2.36 a.u., and mass loss percentages between 42.80-46.35%, suggesting that they are not efficient options for obtaining cellulose microfibers. Furthermore, these experiments are characterized by having at least two factors at the low level. Intermediate absorbance values between 2.70-2.99 a.u. and mass losses between 50.60-53.10% are found in experiments 3, 5 and 7, which belong to Group 2. These results are an indication that this group is a good candidate for the extraction of cellulose microfibers. However, it is important to highlight that this set of experiments has only one factor at a low level. Finally, experiment 8, which has all the factors at a high level, 8% NaOH, 100 °C and 120 min, is the one with the highest absorbance (3.49 a.u.) and a mass loss of 54.30%. This means that, under these conditions, the most effective removal of non-cellulosic material from RH occurs.

One experiment was selected from each of the previously established groups (experiments 1, 3 and 8) and their UV-Vis spectra are shown in Figure 1 (b). It has been reported in the literature that the maximum absorption of the visible spectrum of lignin occurs in two wavelength regions.[46] The first, related to the unconjugated phenolic groups, occurs between 280 and 285 nm, which is not consistent with the results presented in Figure 1 (b). However, according to Mansaray *et al*.,[39] this phenomenon is normal. It is related to the hypochromic effect of NaOH, which causes peaks to shift towards shorter lengths between 214 and 222 nm. The second is representative of the conjugated phenolic groups and is located between 345 and 350 nm. This is in agreement with the results obtained. These results show that the alkaline treatment effectively removes non-

cellulosic components. The three curves in Figure 1 (b) show the same pattern, but with variations in amplitude. In accordance with the Beer-Lambert law, there is a relationship between the absorption of light and the concentration of a material in a solution, the distance travelled and the extinction coefficient.[47] The observed changes are directly related to the concentration of non-cellulosic components present in the supernatant of the alkaline treatment. Therefore, experiment 8 corresponds to the most efficient one for the removal of lignin from RH, using 8% NaOH, 100 °C and 120 min as reaction conditions.

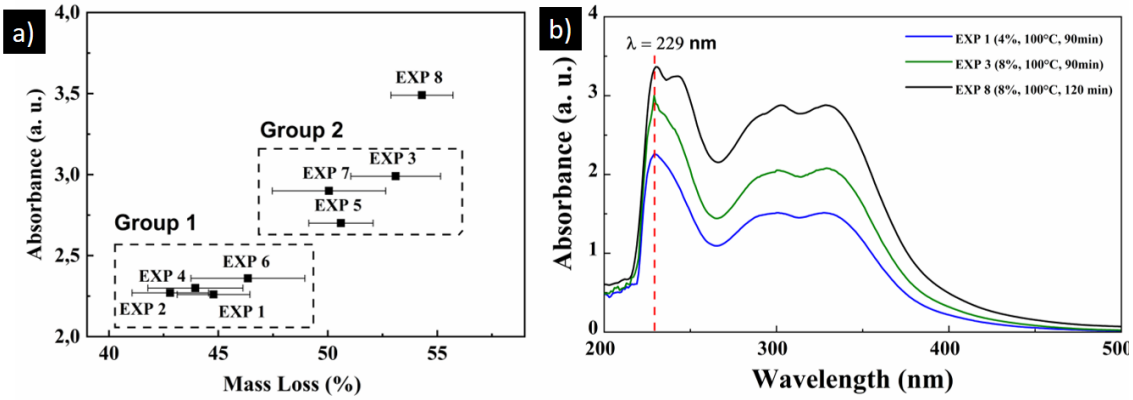

Figure 1: a) Relationship between absorbance and mass loss percentage, and b) UV-Vis spectra of selected experiments

The potential for simultaneous recovery of all lignocellulosic fractions has recently attracted the interest of researchers. Biorefinery processes have been reported in the literature using coagulation, precipitation and centrifugation to extract hemicelluloses, lignin and silica from RH.[53] However, this is not the aim of this work.

Scanning electron microscopy (SEM)

The changes in RH, alkali-treated RH and cellulose microfibers after each chemical treatment stage can be observed from the visual analysis in Figure 2. Initially, the raw RH (Fig. 2a) has a brown colour; however, after the alkaline treatment, its colour becomes brownish-orange (Fig. 2b). In addition, the bleached material (Fig. 2c, d) is different and has a completely white appearance. These colour changes are due to the partial removal of non-cellulosic components, silica and impurities, such as pectin and wax, during the chemical treatment of RH.[25] The second wash in the bleaching process (Fig. 2d) makes the cellulosic microfibers finer compared to the first wash (Fig. 2c).

The morphological changes on the surface of the samples were studied by means of scanning electron microscopy. By comparing the SEM micrographs of raw and alkali-treated RH and extracted cellulose microfibers, shown in Figure 3, the effect of alkali and bleaching treatment on cellulose purification was evaluated. The initial arrangement of the components on the raw RH surface is shown in Figure 3 (a). It can be observed that the sample has a high degree of organization and homogeneity, with a flat surface resembling smooth unidirectional sheets. The non-cellulosic components extend over the entire surface and their function is to provide a protective layer and maintain the structure. A matrix in which cellulose is stored is formed by hemicelluloses and lignin. The structure generally has cellular spaces covered with pectin, silica and waxes; at the ends, they tend to form spherical and spongy agglomerates.[28,29] Silica crystalline bumps cover almost the entire surface of the RH fibres. They form linear ridges and grooves, giving the surface a stiff texture. Silica is responsible for giving the rice husk a rough structure. It is therefore found in the most superficial areas in the form of crystals.[33]

On the other hand, Figure 3 (b) shows the alkali-treated RH, which has a more irregular surface due to the loss of many non-cellulosic components, especially hemicelluloses, silica, pectins, waxes and, to a lesser extent, lignin, by the sodium hydroxide treatment. The initial rice husk sheet (Fig. 3 (a)) had a more uniform structure, but after the alkaline treatment the structure now appears much rougher, porous and swollen; it is also composed of highly cohesive cylindrical structures, which is due to the binding capacity of the unremoved lignin.[30,38]

In addition, similar cracks may be related to the elimination of silica crystals, as reported by Saadiah *et al*.,[28] which suggests that they can be removed by this treatment.

Figure 2: Images of (a) raw, and (b) alkali-treated rice husk; and cellulose after (c) the first wash and (d) the second wash

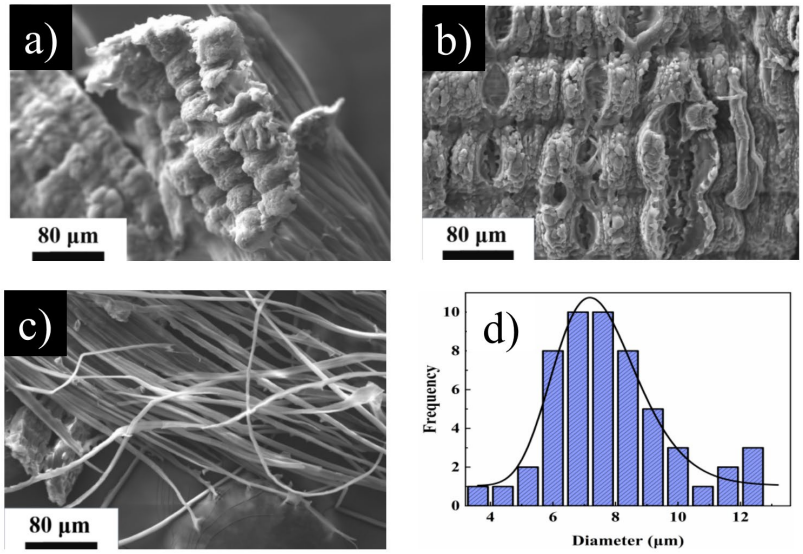

Figure 3: SEM images of (a) raw, and (b) alkali-treated rice husk; and (c) cellulose microfibers; (d) histogram of the diameter of cellulose microfibers

Finally, Figure 3 (c) shows the micrograph of cellulose microfibers obtained after the first bleaching treatment; the fibres are cylindrical and have a cotton-like texture. During this chemical treatment, the bundles are separated into fibres of different diameters, between 4 and 12 µm, as shown in Figure 3 (d). This indicates that a large percentage of non-cellulosic material has been removed and that the bleaching is effective.[38] Sodium hypochlorite can cleave the aromatic rings of lignin and their respective residues by the oxidative action, resulting in the morphological changes described above. In the case of acetic acid, it maintains the pH during the reaction.[30] These results are consistent with those of other reported studies, showing that the sodium hydroxide treatment increases the surface area of the RH, allowing better bleaching action by exposing the microfibres.[33]

As previously shown, the action of sodium hypochlorite and acetic acid continues to delignify the RH. Cylindrical cellulose

microfibres of different diameters were obtained after this treatment. From Figure 3 (c) and processing in ImageJ, the diameter of these microfibres could be determined. The corresponding histogram is shown in Figure 3 (d). As can be seen, the data fit a log-normal probability distribution with an R-squared value of 0.95, with a mean diameter of 7.42 ± 0.12 µm.

The experimental conditions with the lowest and highest mass removal yields were compared to evaluate the efficiency of the alkaline treatment conditions in the delignification process of rice husk. Micrographs of the alkali-treated husk under the conditions of experiment 4 (see Table 4) are shown in Figure 4 (a, b). As discussed above, experiment 4 was one of the least efficient in terms of mass removal during the alkaline treatment. In this experiment, two of its factors were at a low level (temperature at 80 °C and time at 120 min) and the mass removed was 43.95 ± 2.17%.

Experiment 8, where the three factors were at a high level, corresponds to the most favourable conditions for promoting the removal of other components present in the biomass. However, the mass removed in this case was 54.30 ± 1.92%. It is clear that the structure of the alkali-treated husk in Figure 4 (a, b) is much less porous, more uniform and smoother than the structure presented in Figure 4 (c, d). Although the alkali-treated sample has greater porosity and structural destruction under the conditions of experiment 8, this indicates that it has removed a greater amount of surface waxes, pectins and fats, as well as silica, hemicelluloses and lignin under the conditions of this alkaline treatment.

Similarly, in the delignification of alkali-treated RH, the efficiency of different experimental conditions in the bleaching process was evaluated. In this sense, the morphology of the bleached husk obtained with a single washing process was compared with the experimental conditions with lower and higher yields. Figure 5 (a, b) shows the micrographs obtained from the single-washing samples exposed to the conditions of experiments 4 and 5, respectively (see test conditions in Table 3). As previously reported, experiment 4 was the most efficient in removing mass during bleaching. In this experiment, all three factors were at a high level and the mass removed was 59.80 ± 2.26%.

Experiment 5 corresponds to the least efficient conditions for promoting the removal of other components present on the cellulose fibers. In this case, the mass removed was 39.60 ± 3.31%.

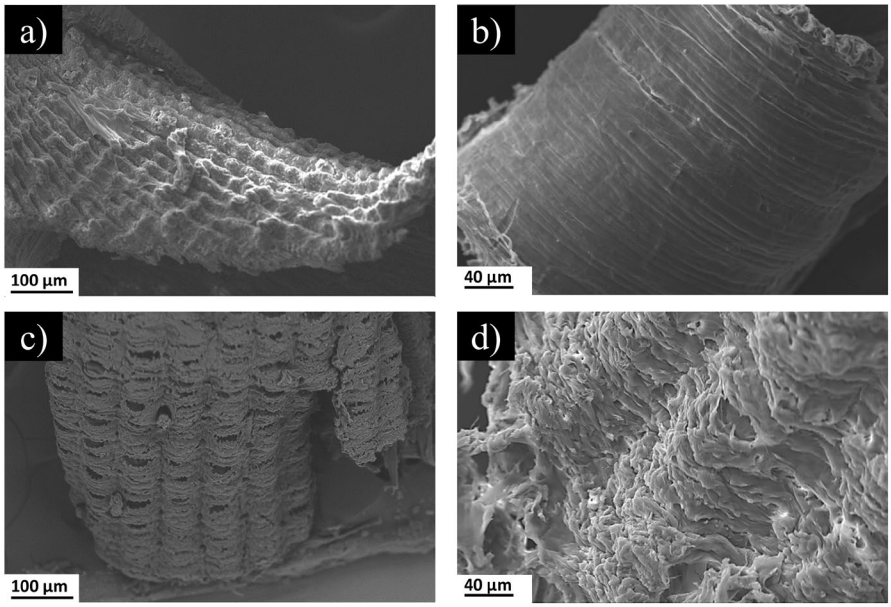

Figure 4: Morphology of rice husk, a) Experiment 4 at 150X, b) Experiment 4 at 320X, c) Experiment 8 at 150 X and d) Experiment 8 at 320X.

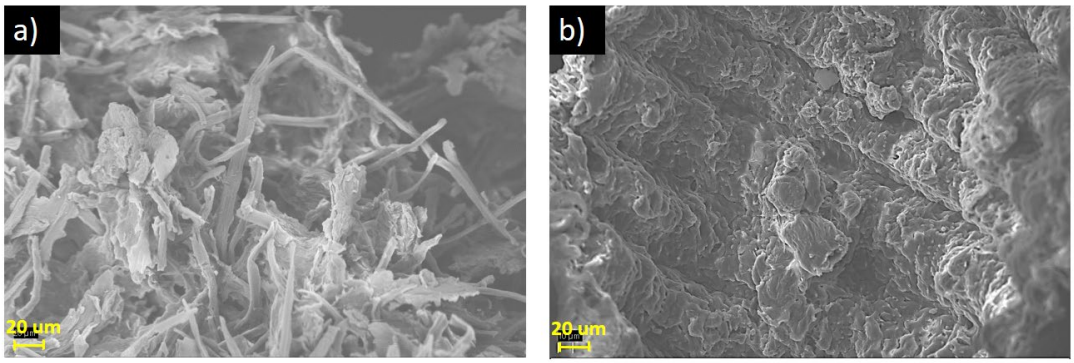

Figure 5: Micrographs of bleached husk samples obtained in the first wash, (a) experiment 4 and (b) experiment 5

The sample in Figure 5 (a) shows a higher degree of defibrillation and some cellulose fibres can be observed in the structure whose sizes are around 10 µm. On the other hand, the sample in Figure 5 (b) presents a more compact structure, this indicates that the conditions of this chemical treatment have not completely favoured the elimination of lignin and hemicelluloses present in the structure, under these conditions the appearance of cellulose fibres is not yet detected.

Thermogravimetric analysis (TGA)

Thermogravimetric analysis (TGA) was performed to assess the thermal stability of both untreated and chemically treated RH fibers. Figure 6 shows the TG and the corresponding derivative curves (DTG) obtained for untreated, alkali-treated and bleached RH. The measurements correspond to the mass changes of the sample upon continuous heating until 600 °C. The blue TG curve in Figure 6 shows the percentages of mass losses as the temperature increases. Moreover, the red DTG curve allows delimiting the characteristic events of the thermal degradation of the samples.

According to studies, the lignocellulosic components present in RH decompose thermally in a temperature range from 150 °C to 500 °C. Specifically, cellulose degrades between 175 °C and 350 °C, hemicelluloses – between 150 °C and 350 °C, and lignin – between 250 °C and 500 °C.[39] Lignin presents a wider decomposition range because, in its structure, there are phenolic groups, which require more thermal energy to break the double bonds of its molecular structure.[38]

The pattern of thermal degradation of RH is associated with three characteristic events. The first goes from room temperature to 100 °C, due to the evaporation of water present in the fiber due to the adsorption effect or surface tension.[28,38,39] Active pyrolysis is the second event between 184-380 °C and corresponds to eliminating hemicelluloses and cellulose. The third event, the passive pyrolysis zone, is related to lignin degradation and occurs in the temperature range from 360 °C to 500 °C.[39] Above 500 °C, the mass loss tends to be constant. This behavior is because only the inorganic part of the material is available, in this case, silica-rich ash.[25] According to Figure 6 (a), the DTG curve presents the aforementioned characteristic events, which correlate to the TG temperature ranges and agree with the reported thermal degradation pattern.

Figure 6 (b and c) shows the results of the thermal degradation of the alkali-treated husk and cellulose microfibers, for which similar decomposition zones are evident; however, the amount of mass removed changes depending on the removal of non-cellulosic components as a product of the chemical treatment implemented. The moisture percentage goes from 5.89% of the raw RH to 12.94% in the alkali-treated RH because the material becomes much more porous due to the removal of pectins and fats during alkaline treatment, which leads to more water being stored.[25] The second degradation event begins at 46.08% for the raw RH and ends at 62.31% in the alkali-treated rice husk; this result indicates that the material obtained with the alkaline treatment has a higher cellulose content. The mass percentage in the third deterioration event for the raw RH is 21.18% and for the alkali-treated RH is 8.76%, which is justified, as the alkaline treatment eliminates lignin from biomass, as confirmed by the UV-Vis technique. Finally, the percentage of residues also changes when the alkaline treatment is applied; this suggests that the

inorganic components of the RH had been eliminated.

Figure 6 (c) corresponds to the thermogram of the cellulose microfibers; the results indicate significant changes in the composition of the material obtained after the bleaching process. Initially, the DTG peak correlated with the percentage of lignin content has partially disappeared, which suggests that the use of sodium hypochlorite and acetic acid is effective in removing lignin residues present in alkali-treated fibers, as well as for the defibrillation of cellulose because now the percentage of cellulose material represents 71.63%. On the other hand, the thermograms show that the thermal stability of the alkali-treated RH and the cellulose microfibers are increased compared to the raw RH. The peak associated with the second thermal degradation event for the raw RH occurs at 304.30 °C, while for the alkali-treated RH and cellulose microfibers are 334.82 °C and 323.89 °C, respectively. Additionally, the onset of the second stage of decomposition was increasing at higher temperatures for the analysed samples. It started at 147.09 °C for the rice husk and increased to 195.48 °C and 200.68 °C for the alkali-treated and bleached husk, as seen in the DTG curves in Figure 6.

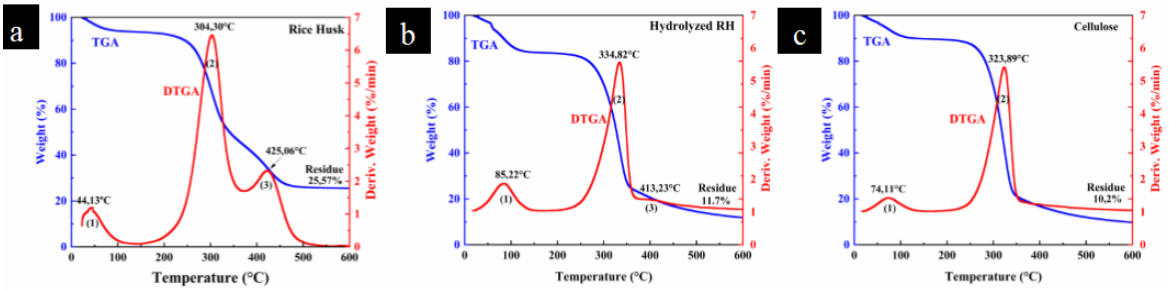

Figure 6: Thermal analysis curves of a) raw RH, b) alkali-treated RH, and c) cellulose microfibers

Table 4
Comparison of thermal behavior of each material after chemical treatments compared with the raw RH

Sample	Mass loss (%)			
	Event 1: Dehydration	Event 2: Hemicellulose and cellulose degradation	Event 3: Lignin degradation	Residues
Raw rice husks	5.89	46.08	21.18	25.57
Alkali-treated rice husks	12.94	62.31	8.76	11.73
Cellulose microfibers	8.21	71.63	7.72	10.30

This phenomenon happens because the non-cellulosic components that degrade at a lower temperature have been removed. These results agree with those of other studies,[25,38,40] and with the SEM analysis presented above, which showed defibrillation during chemical treatments due to removal of non-cellulosic components. Table 4 presents the summarized information related to the mass loss percentages for each of the decomposition events of the material after chemical treatment.

X-ray diffraction (XRD)

One of the lignocellulosic components predominately present in rice husks is cellulose, which has a semi-crystalline structure. This type of polymer is characterized by hydrogen bonds and van der Waals forces that occur between the adjacent crystallites that make it up.[41,42] The XRD analysis was carried out to study the structure and determine the crystallinity index presented by the cellulose microfibers extracted from the RH as the two chemical treatments were implemented. In a previous study,[43] the authors reported that the use of alkali on fibers of vegetable nature eliminates impurities and increases the rigidity of the fibers.

The diffraction patterns and the crystallinity index for the three samples are shown in Figure 7. The typical XRD cellulose pattern presents three peaks at 2θ = 15°–17°, 22.5°, and 35°, and are attributed to the (101), (200), and (004) crystallographic planes.[28] In this study, it is observed that the peaks become narrower and more defined as the chemical treatments are

applied. This behavior coincides with what was reported previously.[8] The highest intensity peak occurs at 2θ = 22.42°, characteristic of cellulose I.[25,28] The crystallinity index was calculated for the materials studied and its values are shown in Figure 7 (b). Chemical treatments increase the crystallinity value, as can be seen in Figure 7 (b); this result is associated with partial elimination of amorphous components, such as lignin and hemicelluloses[26] present in the RH. Cellulose microfibers have the highest crystallinity index.[33,29] This result is because, during alkali treatment, the hydronium ions penetrate the amorphous regions of the cellulose. As a result, the glycosidic bonds are broken, and the individual crystallites are organized;[30] hydrogen bonds also increase.[33] These results agree with those obtained by SEM and TGA, confirming that chemical treatments eliminate amorphous components in the material, increasing the crystallinity of cellulose microfibers.[41] Furthermore, the increase in the crystallinity of cellulose microfibers provides better mechanical properties in terms of hardness and rigidity. Therefore, the cellulose microfibers obtained might be considered as a potential reinforcing material for polymeric matrices.[25]

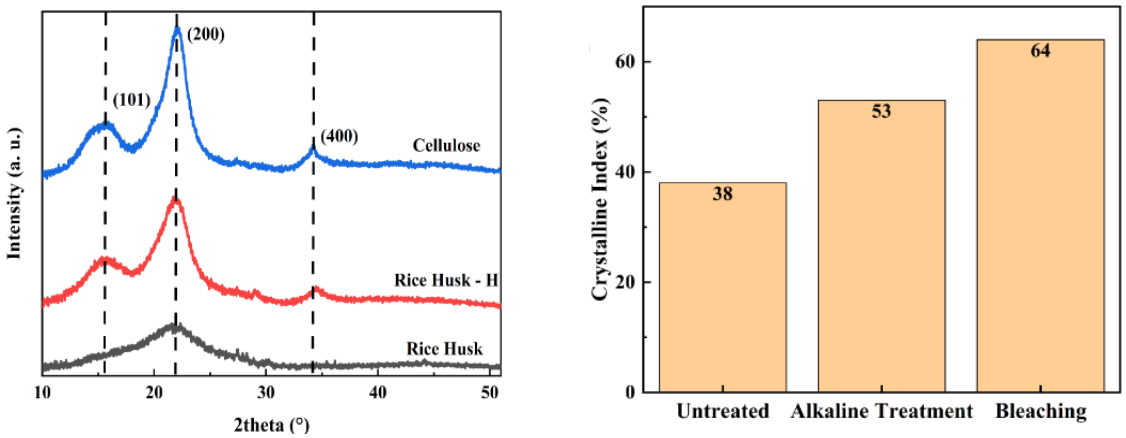

Figure 7: X-ray diffraction patterns (left) and crystallinity index (right) of raw, alkali-treated and bleached RH

Fourier Transform Infrared Spectroscopy (FTIR)

FTIR helps to identify the changes in composition that the RH undergoes as it is subjected to chemical treatments, *i.e.*, with these results, it is possible to evaluate the effectiveness of the processes. In this case, the absorbance peaks in the spectrum will be associated with the functional groups of cellulose, lignin, hemicelluloses, and silica. The obtained spectra of the crude and alkali-treated RH and the cellulose microfibers are shown in Figure 8, and the peaks are listed in Table 5.

In the FTIR spectra, there are two main absorption bands with the most significant peaks. The first ranges from 2850 to 3340 cm^{-1} and the second is between 790 and 1670 cm^{-1}; as stated previously,[29] these bands are consistent with results from the literature. The broadest absorption peak is between 2258 and 3336 cm^{-1} associated with the vibrational stretching mode of the OH group,[26] while the peak between 2895 and 2905 cm^{-1} corresponds to the C-H group with a stretching mode.[49] Both peaks are representative of cellulose, which is why they are present in the three spectra. The same happens with the absorbance peak related to humidity between 1640 and 1670 cm^{-1}.[48]

On the other hand, two typical absorbance peaks related to aromatic rings belonging to the structure of lignin can be observed, the first is between 1590 and 1605 cm^{-1} due to its skeletal vibration,[33] and the second due to a vibrational stretching mode of the C=C bond at 1517 cm^{-1}.[29] Moreover, hemicelluloses are characterized by having a C=O bond with a stretching mode that, in this case, is located between 1725 and 1735 cm^{-1}.[48] The Si-O bond was observed at 792 cm^{-1} with a bending mode.[50] It is important to mention that the previous peaks do not appear in the cellulose microfiber spectrum, indicating that the alkaline treatment with sodium hydroxide and bleaching with sodium hypochlorite can remove non-cellulosic compounds from the RH. In the same way, this result agrees with what was exposed in the findings of UV-Vis, SEM, TGA, and XRD analyses.

Seven more absorbance peaks in the range from 890 to 1430 cm^{-1} have been recognized for cellulose, which are present in all FTIR spectra.

The first one is located between 894 and 898 cm^{-1}, and is associated with the vibration of the glycosidic bonds.[29] Another appears between 1020 and 1032 cm^{-1} due to the skeletal vibration of the C-O-C bond present in the pyranose ring.[26] The peak of the C-C bond occurs in a range that oscillates between 1153 and 1160 cm^{-1} due to a stretching vibration mode of the cellulose rings. In the same way, it happens with the peak of the C-H-C bond located between 1317 and 1337 cm^{-1}. The -CH2 bond with a scissor vibration mode, due to the crystalline integrity in the cellulose structure, has its peak between 1422 and 1429 cm^{-1},[33] and the last one has it in the range of 1368 and 1370 cm^{-1} related to hydrogen bonds.[48]

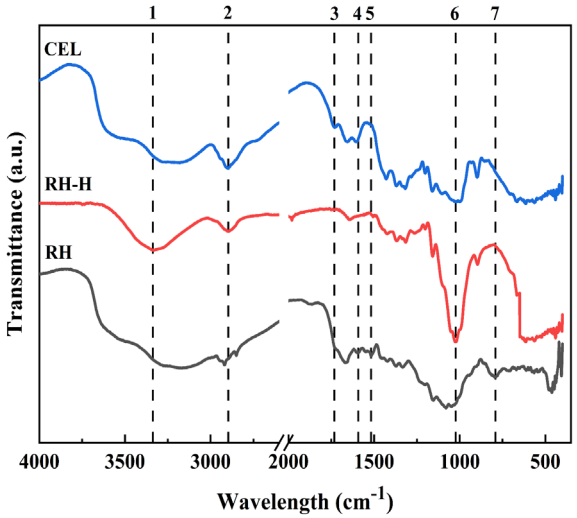

Figure 8: Fourier transform infrared spectroscopy of raw rice husk (RH), alkali-treated rice husk (RH-H) and cellulose microfibers (CEL)

Table 5
Characteristic bands in FTIR of the raw and alkali-treated RH, and cellulose microfibers

Peak	Rice husk characteristic bands, cm^{-1}			Functional group	Associated with	Reference
	Raw	Alkali-treated	Bleached			
1	3258	3263	3336	-OH	Cellulose	[26], [48]
2	2918	2901	2897	C-H	Cellulose	[29], [26], [48], [50]
N/A	1666	1655	1644	Water absorption	Humidity	[25], [48]
4	1593	1603	-	Scent ring	Lignin	[33]
N/A	1422	1429	1425	-CH2	Cellulose	[33], [48]
3	1732	1727	-	C=O	Hemicelluloses	[29], [33], [48]
5	1517	-	-	C=C	Lignin	[29], [48]
N/A	1370	1370	1368	H-bond	Cellulose	[48]
N/A	1337	1317	1315	C-H-C	Cellulose	[48]
N/A	1153	1160	1158	C-C	Cellulose	[48]
6	1031	1020	1024	C-O-C	Cellulose	[26], [48]
N/A	894	897	896	Glycosidic bonds	Cellulose	[29], [33], [48]
7	792	-	-	Si-O	Silica	[48]

Optimization of parameters

Analysis of variance (ANOVA) allowed the study of the effect of process conditions (concentration, time and temperature) of the alkali treatment and bleaching processes, mainly the effect of factors and levels on mass loss (Eq. 2). The chemical process is more efficient when the mass loss associated with the removal of lignin and hemicelluloses is higher. In other words, a better purity of the cellulose microfibres will be

obtained. In order to perform the ANOVA, the data must fulfill three assumptions: independence of the data, homoscedasticity and normality. Finally, to confirm the normality assumption more formally, the Shapiro-Wilks test is performed. The null hypothesis for the test is that the distribution of the data is normal, and the alternative hypothesis is that it is not, with a statistical significance of 5%. The p-value for the alkaline treatment is 0.30 and for the bleaching treatment it is 0.25. It can be concluded that the data are normal in both cases.

Alkaline treatment

In the first stage, a complete factorial design model for alkaline treatment with three controllable factors was developed (Table 1). Figure 9 shows the normal probability plot of the effects of alkaline treatment factors. When a factor moves away from zero, it is considered statistically significant (in Figure 9 the significant factors are represented with a square). On the other hand, a factor can have a positive effect if the response variable increases when it goes from a low level to a high level, that is, it favors the elimination of mass in the alkaline treatment. However, the effect is negative when the response decreases, while the same transition is being made, that is, it favors the elimination of mass in the process. Additionally, if the p value of the variables analyzed is less than 0.05, it is considered statistically significant. The results showed that the most significant factors for this analysis are A: sodium hydroxide concentration, B: temperature and C: reaction time, since they are further from the origin in the graph of standardized effects (see Fig. 9) and the p-value is much less than 0.05; additionally, the double AB interaction is also considered significant.

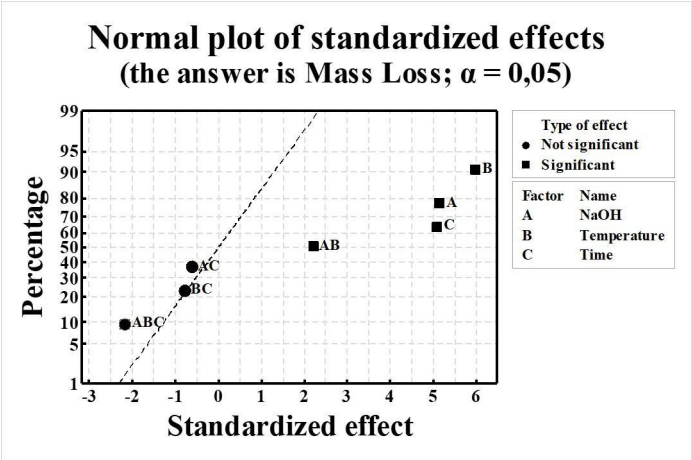

Figure 9: Normal probability chart of standardized effects for alkaline treatment (α = 0.05), where A: sodium hydroxide concentration, B: time and C: temperature

The main effects plots for the alkaline treatment are found in Figure 10 (a, b and c). A factor is considered significant when the line joining the response variable calculated at the low level with the high level is not horizontal; that is, it presents a certain slope. In addition, the order of importance of the factors can be determined, the greater the slope of the said line, the greater the influence of the factor on the response variable. According to the above, the most significant factor in the alkaline treatment is temperature, since it presents a $p=3.66\times10^{-6}$ and, as observed in Figure 10 (b), is the one with the greatest slope. It is possible that the temperature favors the kinetics of the chemical reactions carried out during the alkaline treatment, that is, these reactions can occur more quickly at higher temperatures. In addition, lignin and hemicelluloses are more soluble in alkaline solutions at high temperatures and the activation of chemical agents (NaOH) is favored, which can facilitate their removal from rice husk. Additionally, at high temperatures, it is clear that the kinetic energy increases and can break the chemical bonds present in the lignin and hemicellulose structure, which facilitates their disintegration and elimination.[51] As previously mentioned, it is again confirmed that the percentage of mass loss is maximized when the three factors are at a high level, in this case, a concentration of 8% sodium hydroxide, a time of 120 min and a temperature of 100 °C, which

correspond to the conditions of experiment 8 (see Table 2).

In Figure 10 (d-f), the graphs of double interactions of the alkaline treatment factors are presented. The double interaction is significant if the lines approach each other or intersect at some point (Fig. 10 (d)), which in this case corresponds to the interaction between the sodium hydroxide concentration and temperature (p-value of 0.04). On the other hand, the double interaction is not significant if the lines represented in the graph tend to be parallel (Fig. 10 (e, f)). The double interactions between base concentration and reaction time (p-value of 0.53) and between temperature and reaction time (p-value of 0.43) are not significant in this model.

When the interactions that do not contribute significantly to the statistical model are eliminated, that is, AC, BC and ABC, Equation 3 is obtained, which only includes both the factors and the significant interactions in the alkaline treatment:

$$\% \text{ mass loss} = 48.241 + 2.109*A + 2.453*B + 2.084*C + 0.897*AB \quad (3)$$

Table 6 shows the ANOVA of the refined model for the alkaline treatment. In this, the R-square is 79.53%. The preceding indicates that for this treatment, there is a reliable relationship between the experimental and theoretical values, which is verified through the analysis carried out for the mass loss percentage during the alkaline treatment, where it was observed that the relative error did not exceed 2% (data not shown).

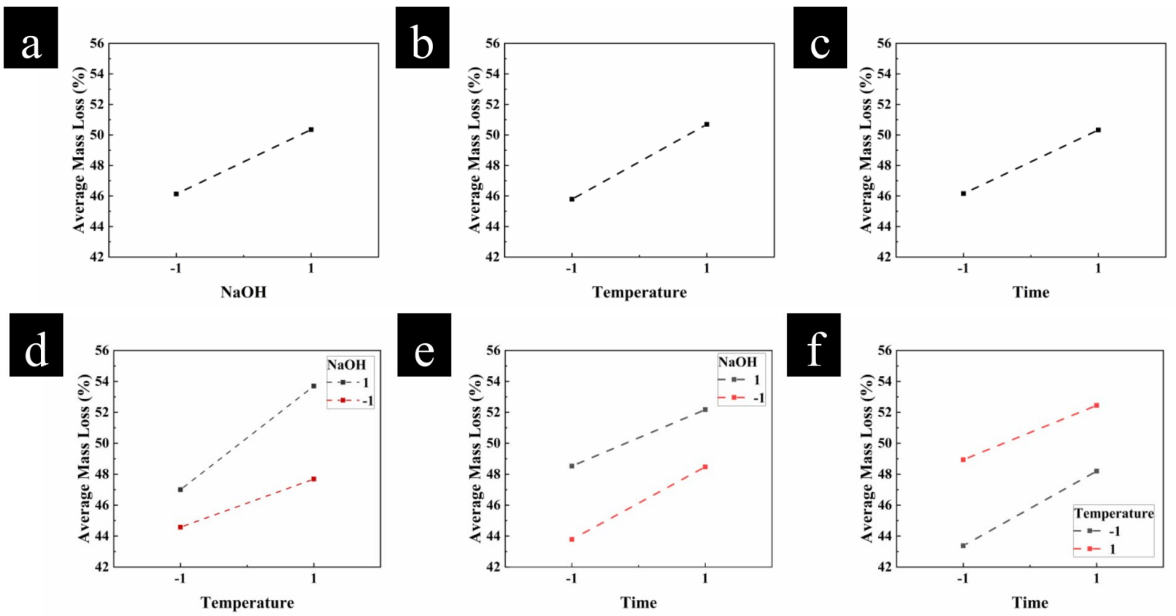

Figure 10: Graphs of main effects for the mass loss percentage of the alkaline treatment: a) concentration of sodium hydroxide, b) temperature and c) time; and double interaction graphs for: d) temperature - sodium hydroxide concentration, e) time - sodium hydroxide concentration and, f) time – temperature (coded values)

Table 6
ANOVA of the optimized model for the alkaline treatment

Factor	DF	Sum of Squares	Mean Square	F Value	P Value
NaOH	1	142.383	142.383	27.38	1.82×10^{-5}
Temperature	1	192.57	192.57	37.03	1.98×10^{-6}
Time	1	139.028	139.028	26.73	2.15×10^{-5}
NaOH * Temperature	1	25.74	25.74	4.95	3.45×10^{-3}
NaOH * Temperature * Time	1	25.74	25.74	4.95	3.45×10^{-5}
Model	5	525.462	105.092	20.21	3.3×10^{-8}
Error	26	135.216	5.201		

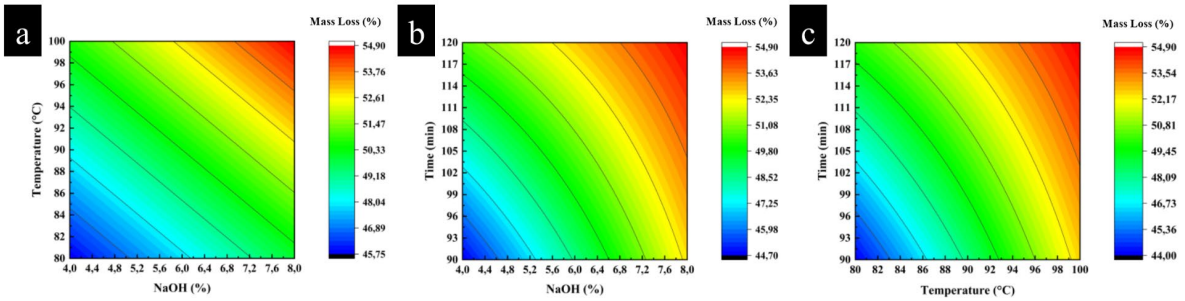

Figure 11: Response surface plots of the percentage of mass loss of the alkaline treatment as a function of a) concentration and temperature, b) time and concentration, and c) time and temperature

In general, contour graphs or response surfaces are usually very appropriate for optimization processes, since they allow us to study the behavior of the interaction of the factors and their effect on the response variable and thus identify their importance in the model, as well as to find those conditions where the response variable is maximized.[52] Figure 11 shows the contour plots of percent mass loss as a function of alkaline treatment factors. The percentage of mass loss is maximized (red color in the graph) when each of the factors is at a high level, that is, when the sodium hydroxide concentration is 8%, the time is 120 min and the temperature is 100 °C. These results are in agreement with what was found with the UV-Vis technique.

Bleaching treatment

ANOVA was also performed for the bleaching treatment. In the case of bleaching, factors A, B, and C, which are the sodium hypochlorite concentration, temperature, and time, respectively, and the BC interaction are the most significant. Except for the triple interaction, the others have a positive effect, and factor A has the most significant magnitude, as seen in Figure 12.

Figure 13 (a-c) shows the effects of the main factors for the percentage of mass loss in bleaching, where it is evident that these are ordered in ascending order according to their importance, such as the concentration of sodium hypochlorite (p-value of 1,77 x 10^{-10}), time (p-value of 1.80 x 10^{-7}) and temperature (3.8 x 10^{-5}). Additionally, it can be observed that the mass loss percentage is maximized when the factors are at their highest levels; in this case, a concentration of sodium hypochlorite and acetic acid at 2.3%, time of 60 min, and temperature of 90 °C, which correspond to the conditions of experiment 4.

On the other hand, the plots in Figure 13 (d-f) represent the double interaction graphs for the mass loss percentage in bleaching. In them, it can be observed that the time-temperature interaction (Fig. 13 (f)) is significant because the response variable presents dynamic changes when the two factors are at their different levels; it also has a p-value of 5.74 × 10^{-4}.

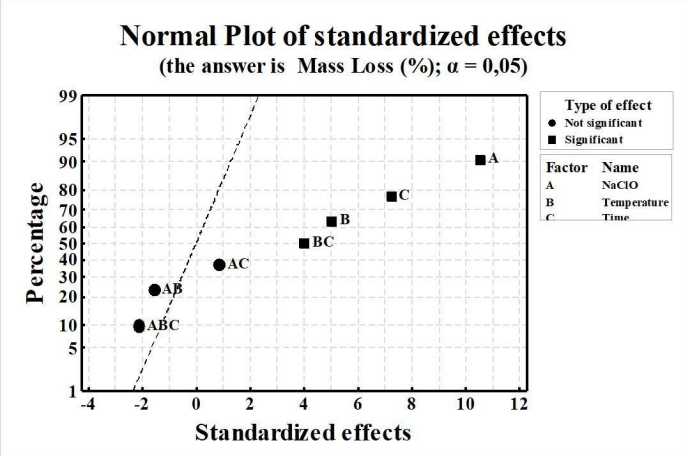

Figure 12: Normal probability chart of standardized effects for bleaching (α = 0.05), where A: sodium hypochlorite concentration, B: temperature and C: time

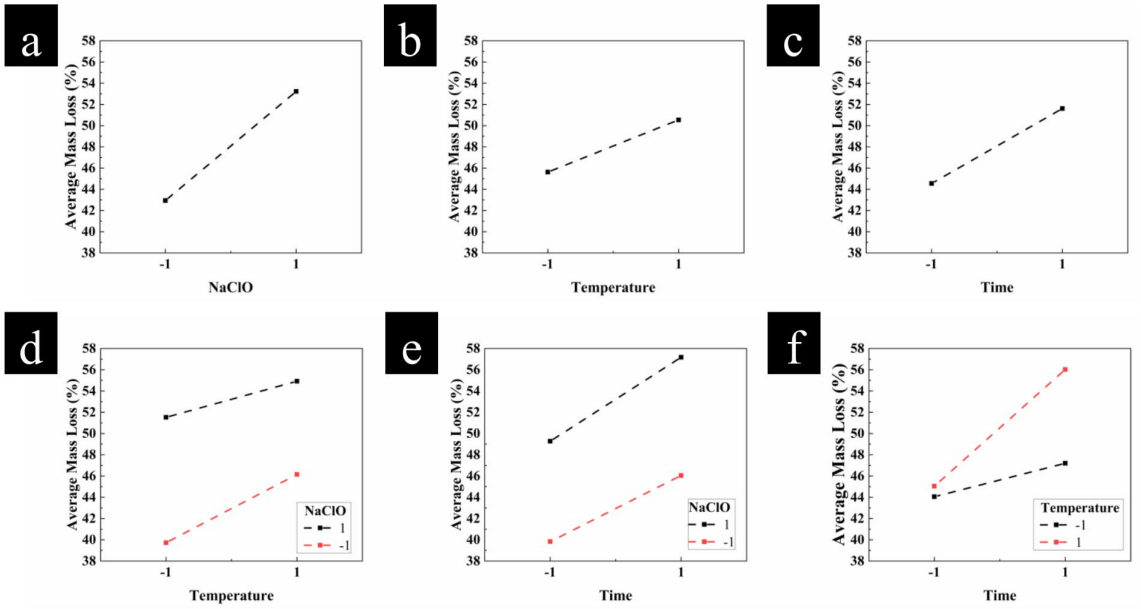

Figure 13: Main effects plots for percent mass loss of bleaching for a) sodium hypochlorite concentration, b) temperature, and c) time; and interaction graphs for mass loss percentage of bleaching d) temperature - sodium hypochlorite concentration, e) time - sodium hypochlorite concentration and f) time - temperature

Table 7
ANOVA of the optimized model for bleaching

Factor	DF	Sum of Squares	Mean Square	F Value	P Value
Concentration	1	846.66	846.66	94.82	2.51×10^{-10}
Temperature	1	193.06	193.06	21.62	7.81×10^{-05}
Time	1	399.03	399.03	44.69	3.56×10^{-07}
Temperature * Time	1	122.46	122.46	13.71	9.65×10^{-04}
Model	4	1561.22	390.30	43.71	2.04×10^{-11}
Error	27	241.09	8.93	0	0

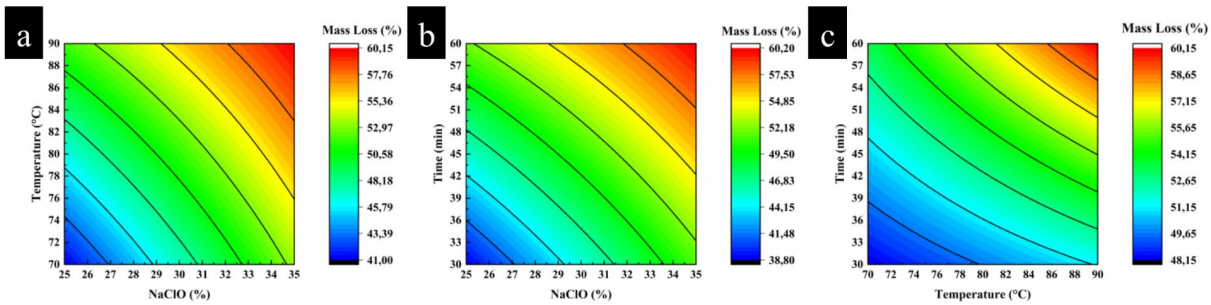

Figure 14: Response surfaces of the mass loss percentage from bleaching as a function of a) concentration and temperature, b) time and concentration, c) time and temperature

Based on the results obtained, the need arises to eliminate the factors or/and their respective interactions that do not contribute significantly to the statistical model. Below is Equation 4 associated with bleaching:

$$\% \text{ mass loss} = 48.081 + 5.144*A + 2.456*B + 3.531*C + 1.956*BC \quad (4)$$

where A: sodium hypochlorite concentration, B: temperature, and C: time.

Table 7 shows the ANOVA of the refined model for bleaching. For the second model, the R-square is 86.62%, indicating the reliable relationship between the experimental and theoretical values.

Figure 14 presents to the contour plots for the mass loss percentage from bleaching. According to the results obtained, the response variable is always maximized when the factors are at high

levels, suggesting that the most appropriate conditions are 2.3% sodium hypochlorite, 60 min, and 90 °C, corresponding to the conditions from experiment 4.

CONCLUSION

This study investigated the effectiveness of alkaline treatment and bleaching of rice husks to remove lignin, hemicelluloses and silica ash, while maintaining a high solid yield.

Two chemical treatments, alkaline and bleaching, were used to obtain cellulose microfibres. Ultraviolet-visible spectroscopy, morphological studies by SEM, infrared spectroscopy and X-ray diffraction analysis confirmed the elimination of non-cellulosic materials. This led to an increase in the crystallinity index from 38% to 64%, and allowed the defibrillation of the cellulose. In addition, compared to the raw rice husk sample, the TGA study showed that the fibres have a higher thermal stability. The microfibres obtained had an average size of 7.42 ± 0.12 μm, this was corroborated by SEM analysis.

The alkali treatment experiments suggest that keeping the reagent concentration, temperature and time factors at 8%, 100 °C and 120 min, respectively, improves the removal of impurities. For bleaching, in order to maximise the removal of lignin, non-cellulosic components and ashes, the optimised conditions of 2.3% sodium hypochlorite concentration, temperature of 90 °C and time of 60 min are suggested.

ACKNOWLEDGMENTS: The authors thank Universidad Autónoma de Manizales for financial support through project 756-116 at SIUAM. Astrid Lorena Giraldo also thanks CONACYT for the financial support through project 881 from the Mexico program researchers. In addition, this study was partially carried out at CENAPROT and LIDTRA national laboratories from Cinvestav-Queretaro. The authors also thank Reina Araceli Mauricio-Sánchez and Martin Adelaido Hernandez Landaverde for FTIR and XRD measurements and their technical support. The authors also thank to Ivan Gerardo Cely from Rio Gallegos, Argentina, for SEM analysis.

REFERENCES

[1] R. Singh, P. Srivastava, P. Singh, S. Upadhyay and A. S. Raghubanshi, in "Urban Agriculture and Food Systems", IGI Global, 2019, pp. 439–467, https://doi.org/10.4018/978-1-5225-8063-8.ch022

[2] Y. Hsieh, Y. Du, F. Jin, Z. Zhou and H. Enomoto, *Chem. Eng. Res. Des.*, **87**, 13 (2009), https://doi.org/10.1016/j.cherd.2008.07.001

[3] S. Uniyal, R. Paliwal, B. Kaphaliya and R. K. Sharma, in "Megacities and Rapid Urbanization", IGI Global, 2020, pp. 20–30, https://doi.org/10.4018/978-1-5225-9276-1.ch002

[4] M. Urbina-Fuentes, L. Jasso-Gutiérrez, R. Schiavon-Ermani, R. Lozano and J. Finkelman, *Gaceta de México*, **153** (2019), https://doi.org/10.24875/gmm.m18000059

[5] M. G. R. Cannell, in "Planted Forests: Contributions to the Quest for Sustainable Societies", Dordrecht, Springer Netherlands, 1999, pp. 239–262, https://doi.org/10.1007/978-94-017-2689-4_17

[6] J. De Tavernier, *J. Agric. Environ. Ethics*, **25**, 895 (2012), https://doi.org/10.1007/s10806-011-9366-7

[7] Y. Li, X. Ding, Y. Guo, C. Rong, L. Wang *et al.*, *J. Hazard. Mater.*, **186**, 2151 (2011), https://doi.org/10.1016/j.jhazmat.2011.01.013

[8] A. K. Chapagain and A. Y. Hoekstra, *Ecol. Econ.*, **70**, 749 (2011), https://doi.org/10.1016/j.ecolecon.2010.11.012

[9] S. Muthayya, J. D. Sugimoto, S. Montgomery and G. F. Maberly, *Ann. N. Y. Acad. Sci.*, **1324**, 7 (2014), https://doi.org/10.1111/nyas.12540

[10] Agricultural Market Information System, "Market Monitor February 2023", Feb. 2023, available at: https://www.amis-outlook.org/news/detail/en/c/342591/

[11] DANE, "Encuesta Nacional de Arroz Mecanizado (ENAM)", Bogotá, Boletín Técnico, Feb. 2023

[12] H. Moayedi, B. Aghel, M. M. Abdullahi, H. Nguyen and A. Safuan, *J. Clean. Prod.*, **237**, 117851 (2019), https://doi.org/10.1016/j.jclepro.2019.117851

[13] N. Radenahmad, N. Morni, A. Ahmed, M. Abu Bakar, J. Zaini *et al.*, in Procs. *7th Brunei International Conference on Engineering and Technology 2018* (*BICET 2018*), 2018, https://doi.org/10.1049/cp.2018.1527

[14] J. F. Velasco-Muñoz, J. A. Aznar-Sánchez, B. López-Felices and I. M. Román-Sánchez, *Sustain. Prod. Consum.*, **34**, 257 (2022), https://doi.org/10.1016/j.spc.2022.09.017

[15] D. Klemm, B. Heublein, H. Fink and A. Bohn, *Angew. Chem. Int. Ed.*, **44**, 3358 (2005), https://doi.org/10.1002/anie.200460587

[16] Y. Feng, H. Cölfen and R. Xiong, *J. Mater. Chem. B Mater. Biol. Med.*, **11**, 5231 (2023), https://doi.org/10.1039/d2tb02611b

[17] M. F. Rosa, E. S. Medeiros, J. A. Malmonge, K. S. Gregorski, D. F. Wood *et al.*, *Carbohyd. Polym.*, **81**, 83 (2010), https://doi.org/10.1016/j.carbpol.2010.01.059

[18] A. Mandal and D. Chakrabarty, *Carbohyd. Polym.*, **86**, 1291 (2011), https://doi.org/10.1016/j.carbpol.2011.06.030

[19] D. Pasquini, E. de M. Teixeira, A. A. da S. Curvelo, M. N. Belgacem and A. Dufresne, *Ind. Crop.*

Prod., **32**, 486 (2010), https://doi.org/10.1016/j.indcrop.2010.06.022
[20] M. K. Mohamad Haafiz, S. J. Eichhorn, A. Hassan, and M. Jawaid, *Carbohyd*. *Polym*., **93**, 628 (2013), https://doi.org/10.1016/j.carbpol.2013.01.035
[21] B. Wang and M. Sain, *Compos*. *Sci*. *Technol*., **67**, 2521 (2007), https://doi.org/10.1016/j.compscitech.2006.12.015
[22] A. Alemdar and M. Sain, *Bioresour*. *Technol*., **99**, 1664 (2008), https://doi.org/10.1016/j.biortech.2007.04.029
[23] E. M. Santos Ventura, M. A. Escalante Álvarez and A. Gutiérrez Becerra, *Emerg*. *Mat*. *Res*., **9**, 1258 (2020), https://doi.org/10.1680/jemmr.20.00073
[24] D. Barana, A. Salanti, M. Orlandi, D. S. Ali and L. Zoia, *Ind*. *Crop*. *Prod*., **86**, 31 (2016), https://doi.org/10.1016/j.indcrop.2016.03.029
[25] N. Johar, I. Ahmad and A. Dufresne, *Ind*. *Crop*. *Prod*., **37**, 93 (2012), https://doi.org/10.1016/j.indcrop.2011.12.016
[26] M. Islam, N. Kao, S. Bhattacharya, R. Gupta and P. Bhattacharjee, *J. Taiwan Inst*. *Chem*. *Eng*., **80**, 820 (2017), https://doi.org/10.1016/j.jtice.2017.06.042
[27] V. Sumi and B. Kandasubramanian, *Eur*. *Polym*. *J*., **160**, 110789 (2021), https://doi.org/10.1016/j.eurpolymj.2021.110789
[28] S. Rashid and H. Dutta, *Ind*. *Crop*. *Prod*., **154**, 112627 (2020), https://doi.org/10.1016/j.indcrop.2020.112627
[29] K. Bhandari, S. Roy Maulik and A. Bhattacharyya, *J*. *Inst*. *Eng*. (*India*): *Series E*, **101**, 99 (2020), https://doi.org/10.1007/s40034-020-00160-7
[30] S. Collazo-Bigliardi, R. Ortega-Toro and A. Chiralt Boix, *Carbohyd*. *Polym*., **191**, 205 (2018), https://doi.org/10.1016/j.carbpol.2018.03.022
[31] D. Barana, A. Salanti, M. Orlandi, D. Ali and L. Zoia, *Ind*. *Crop*. *Prod*., **86**, 31 (2016), https://doi.org/10.1016/j.indcrop.2016.03.029
[32] Islam, N. Kao, S. Bhattacharya, R. Gupta and H. Choi, *Chin*. *J*. *Chem*. *Eng*., **26**, 465 (2018), https://doi.org/10.1016/j.cjche.2017.07.004
[33] H. Hafid, F. Omar, J. Zhu and M. Wakisaka, *Carbohyd*. *Polym*., **260**, 117789 (2021), https://doi.org/10.1016/j.carbpol.2021.117789
[34] P. Lu and Y. Hsieh, *Carbohyd*. *Polym*., **87**, 564 (2012), https://doi.org/10.1016/j.carbpol.2011.08.022
[35] J. George and S. N. Sapathi, *Nanotechnol*. *Sci*. *Appl*., **8**, 45 (2015), https://doi.org/10.2147/nsa.s64386
[36] Minitab, available at: https://support.minitab.com/es-mx/minitab/18/getting-started/designing-an-experiment/
[37] A. Jankovic, G. Chaudhary and F. Goia, *Energ*. *Build*., **250**, 111298 (2021), https://doi.org/10.1016/j.enbuild.2021.111298
[38] R. Khandanlou, G. C. Ngoh and W. T. Chong, *BioResources*, **11**, 3 (2016), https://doi.org/10.15376/biores.11.3.5751-5766
[39] K. G. Mansaray and A. E. Ghaly, *Bioresour*. *Technol*., **65**, 107 (1998), https://doi.org/10.1016/s0960-8524(98)00031-5
[40] X. Chen, J. Yu, Z. Zhang and C. Lu, *Carbohyd*. *Polym*., 85, 245 (2011), https://doi.org/10.1016/j.carbpol.2011.02.022
[41] . N. Megashah, H. Ariffin, M. R. Zakaria, M. A. Hassan, Y. Andou *et al*., *Cellulose*, **27**, 7417 (2020), https://doi.org/10.1007/s10570-020-03296-2
[42] Y.-H. P. Zhang and L. R. Lynd, *Biotechnol*. *Bioeng*., **88**, 797 (2004), https://doi.org/10.1002/bit.20282
[43] L. Y. Mwaikambo and M. P. Ansell, *J*. *Mater*. *Sci*., **41**, 2483 (2006), https://doi.org/10.1007/s10853-006-5098-x
[44] L. Segal, J. J. Creely, A. E. Martin and C. M. Conrad, *Text*. *Res*. *J*., **29**, 786 (1959), https://doi.org/10.1177/004051755902901003
[45] S. A. Lesik, "Applied Statistical Inference with MINITAB" (R), second edition, London, CRC Press, 2021
[46] S. De, S. Mishra, E. Poonguzhali, M. Rajesh and K. Tamilarasan, *Int*. *J*. *Biol*. *Macromol*., 145, 795 (2020)
[47] D. F. Swinehart, *J*. *Chem*. *Educ*., **39**, 333 (1962)
[48] S. Rashid and H. Dutta, *Ind*. *Crop*. *Prod*., **154**, 112627 (2020), https://doi.org/10.1016/j.indcrop.2020.112627
[49] A. M. Das, A. A. Ali and M. P. Hazarika, *Carbohyd*. *Polym*., **112**, 342 (2014), https://doi.org/10.1016/j.carbpol.2014.06.006
[50] M. H. Shahrokh Abadi, A. Delbari, Z. Fakoor and J. Baedi, *J*. *Ceram*. *Sci*. *Technol*., **6**, 41 (2015), https://doi.org/10.4416/JCST2014-00028
[51] A. Bazargan, Z. Wang, J. P. Barford, J. Saleem and G. McKay, *J. Clean. Prod.*, **260**, 120848 (2020), https://doi.org/10.1016/j.jclepro.2020.120848
[52] D. Barana, A. Salanti, M. Orlandi, D. S. Ali and L. Zoia, *Ind*. *Crop*. *Prod*., **86**, 31 (2016), https://doi.org/10.1016/j.indcrop.2016.03.029